JOC The Journal of Organic Chemistry

Article

pubs.acs.org/joc

Thiol-Activatable Triplet−Triplet Annihilation Upconversion with Maleimide-Perylene as the Caged Triplet Acceptor/Emitter

Zafar Mahmood and Jianzhang Zhao*

State Key Laboratory of Fine Chemicals, School of Chemical Engineering, Dalian University of Technology, E-208 West Campus, 2 Ling-Gong Road, Dalian 116024, P. R. China

Supporting Information

ABSTRACT: Efficient thiol-activated triplet−triplet annihilation (TTA) upconversion system was devised with maleimide-caged perylene (**Py-M**) as the thiol-activatable triplet acceptor/emitter and with diiodoBodipy as the triplet photosensitizer. The photophysical processes were studied with steady-state UV−vis absorption spectroscopy, fluorescence spectroscopy, electrochemical properties, and nanosecond transient absorption spectroscopy. The triplet acceptor/emitter **Py-M** shows week fluorescence (Φ_F = 0.8%), and no upconversion (Φ_{UC} = 0%) was observed. The quenching of fluorescence of **Py-M** is due to photoinduced electron-transfer (PET) process from perylene to maleimide-caging unit, which quenches the singlet excited state of perylene. The fluorescence of **Py-M** was enhanced by 200-fold (Φ_F = 97%) upon addition of thiols such as 2-mercaptoethanol, and the Φ_{UC} was increased to 5.9%. The unique feature of this thiol-activated TTA upconversion is that the activation is based on addition reaction of the thiols with the caged acceptor/emitter, and no side products were formed. The previously reported cleavage approach gives side products which are detrimental to the TTA upconversion. With nanosecond transient absorption spectroscopy, we found that the triplet excited state of **Py-M** was not quenched by any PET process, which is different from singlet excited state (fluorescence) of **Py-M**. The results are useful for study of the triplet excited states of organic chromophores and for activatable TTA upconversion.

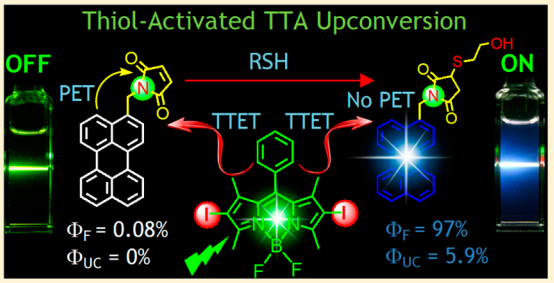

1. INTRODUCTION

Triplet−triplet annihilation (TTA) upconversion has attracted much attention,[1−3] due to its efficient harvesting of the incoherent visible/near IR photoexcitation energy,[4−6] high upconversion quantum yield,[7,8] and the feasibly tunable absorption/emission wavelength.[9−11] Various new triplet photosensitizers and triplet acceptors have been developed for TTA upconversion,[1,2,12−15] and the mechanism has been studied by kinetics modelings.[16−19] TTA upconversion has been used for luminescence bioimaging,[11,20] photovoltaics,[20−22] photocatalysis, or photoinduced drug release,[23,24] etc. In order to add more functionality to TTA upconversion, external stimuli-activatable or switchable TTA upconversion is highly desired, such as light-switchable,[25−27] or chemical-activatable TTA upconversion.[28,29] However, such systems are rarely reported, and much room is left for development of new methods for activatable TTA upconversion.

On the other hand, intracellular thiols, such as glutathione (GSH), are highly important to maintain the normal functionality of the cells, including intracellular redox activities, xenobiotic metabolism, intracellular signal transduction, and gene regulation. As a result, a great amount of fluorescent molecular probes for selective detection of thiol have been developed, and in vivo luminescence imaging of thiols was also studied.[30−35] Following this line, it is interesting to develop thiol-activatable TTA upconversion systems, which are important for luminescence bioimaging of the intracellular thiols and for the development of TTA upconversion.

Recently we developed 2,4-dinitrobenzenesulfonylamide (DNBS)-caged diiodoBodipy as the switchable triplet photosensitizer for thiol-activatable TTA upconversion.[28] Unfortunately, the caging effect of DNBS on the triplet-state yield and the triplet-state lifetime of diiodoBodipy is unsatisfactory. For example, the singlet oxygen quantum yield (Φ_Δ) of the previously reported DNBS-caged diiodoBodipy, as an indication of the triplet-state yield (Φ_T), increased from 74% to 88% in the presence of thiols. The high Φ_Δ value of the caged triplet photosensitizer actually indicated inefficient caging effect by DNBS on the triplet-state formation. As a result, the switching effect of the TTA upconversion is unsatisfactory, and the upconversion quantum yields (Φ_{UC}) only increased from 0.2% to 0.5% in the presence of thiols.[28] Therefore, thiol-activated TTA upconversion with much more significant activation effect is highly desired.

Herein we use a new method to enhance the activation effect of the thiols on the TTA upconversion. We used the maleimide-caged perylene fluorophore **Py-M** (Scheme 1) as the thiol-switchable triplet acceptor/emitter for thiol-activated TTA upconversion. It is well-known that maleimide is an ideal

Received: October 19, 2015
Published: December 22, 2015

DOI: 10.1021/acs.joc.5b02415
J. Org. Chem. 2016, 81, 587−594

Scheme 1. Maleimide-Caged Perylene Fluorophore Py-M[a]

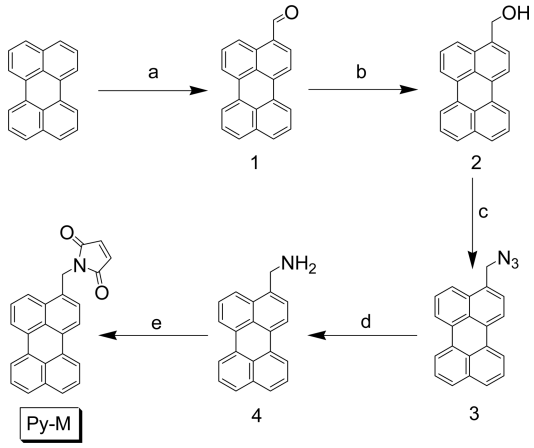

[a]Key: (a) *o*-dichlorobenzene, DMF, $POCl_3$, 100 °C, 4 h; (b) THF, methanol, $NaBH_4$, RT, overnight; (c) **1**. CBr_4, DMF, 10 min. **2**. NaN_3, RT, 24 h; (d) 10% Pd/C, H_2, methanol, RT, 16 h; (e) maleic anhydride, acetic acid, reflux, 6 h.

electron acceptor (caging group) for construction of fluorescent thiol probes.[36,37] Perylene shows high fluorescence quantum yield and has been widely used as triplet acceptor/emitter for TTA upconversion.[1−3] Thus, we devised maleimide-attached perylene **Py-M** (Scheme 1), and it shows very weak fluorescence (Φ_F = 0.8%), thus it was assumed that no upconversion will be observed with **Py-M** as the triplet acceptor/emitter. In the presence of thiols, such as 2-mercaptoethanol, an addition reaction to the aliphatic C═C bond in **Py-M** will occur, the fluorescence is assumed to be enhanced, and as a result, the TTA upconversion may be activated. Indeed we observed the anticipated thiol-activated TTA upconversion. The photophysical processes were studied with steady-state and time-resolved spectroscopies.

2. RESULTS AND DISCUSSION

2.1. Design and Synthesis of the Compounds. The molecular structure designing rational of **Py-M** is that attachment of the maleimide moiety to the perylene (a fluorophore, widely used as triplet acceptor/emitter in TTA upconversion previously)[18] will quench the fluorescence, via photoinduced electron transfer (PET).[38] Reaction of **Py-M** with thiols, such as 2-mercaptoethanol, will probably switch on the fluorescence of **Py-M** as well as the TTA upconversion. Herein the reaction product is without any electron withdrawal features, thus the undesired quenching of the triplet state (as well as the TTA upconversion) by the reaction product of the previously reported DNBS-caged photosensitizer was eliminated.[28] In that method, the thiol-cleavage product shows quenching effect on the triplet excited state of the photosensitizer, and as a result, the TTA upconversion was detrimented.[28]

2.2. UV−vis Absorption and Fluorescence Emission Spectra. The UV−vis absorption spectra of the compounds were studied (Figure 1). The absorption of **Py-M** is slightly reduced, and the absorption wavelength is red-shifted as compared with that of perylene, which is probably due to the substitution effect. In the presence of 2-mercaptoethanol, the UV−vis absorption does not give any changes, which is reasonable since the perylene π-conjugation framework was not perturbed by the thiol addition. We also confirmed that the

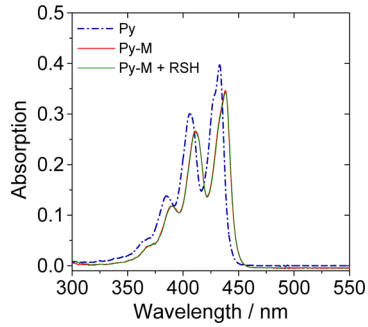

Figure 1. UV−vis absorption spectra of **Py**, **Py-M**, and **Py-M** + 200 equiv 2-mercaptoethanol (RSH). $c = 1.0 \times 10^{-5}$ M in MeOH, 20 °C.

UV−vis absorption spectrum of perylene did not change in the presence of 2-mercaptoethanol (Figures S12 and S13, Supporting Information).

The fluorescence emission property of **Py-M** was studied (Figure 2). In stark contrast to the strongly fluorescent perylene

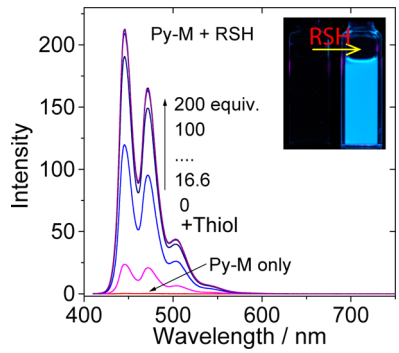

Figure 2. Fluorescence emission of **Py-M** in the presence of 2-mercaptoethanol (λ_{ex} = 406 nm). $c = 1.0 \times 10^{-5}$ M in MeOH, 20 °C . The absorption at the excitation wavelength is same for all the solutions.

(**Py**, Scheme 2) (Φ_F = 94%), **Py-M** shows no fluorescence in the absence of thiols (Φ_F = 0.8%). With addition of 2-mercaptoethanol, the fluorescence was greatly intensified (Figure 2). For perylene, however, no fluorescence enhancement was observed in the presence of thiols (Figures S14 and S15, Supporting Information). These results indicate that thiol adduction to the maleimide moiety switches on the

Scheme 2. Activation Mechanism of the Thiol-Activatable TTA Upconversion with Maleimide-Caged Triplet Acceptor/Emitter[a]

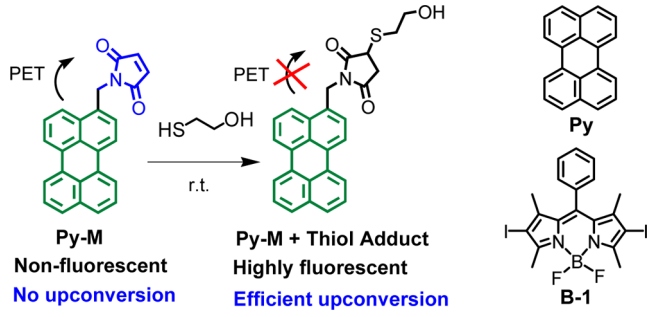

[a]**B-1** is triplet photosensitizer, perylene (**Py**) is reference acceptor, and **Py-M** + Thiol adduct used in this study.

DOI: 10.1021/acs.joc.5b02415
J. Org. Chem. 2016, 81, 587−594

fluorescence of fluorophore perylene.[36,37] The reaction was confirmed by HR MS analysis of the reaction mixture (Figures S16 and S17, Supporting Information). The fluorescence quantum yield (Φ_F) of **Py-M** was determined as 97% in the presence of 2-mercaptoethanol (Figure 2).

The fluorescence lifetimes of **Py-M** in the absence and presence of thiols were studied with the TCSPC technique (Figure 3). In the absence of thiols, **Py-M** gives a fluorescence

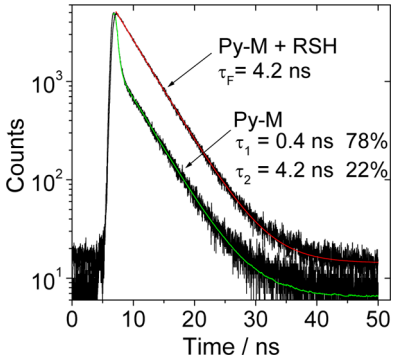

Figure 3. Decay traces of the fluorescence of **Py-M** and that after addition of 200 equiv of 2-mercaptoethanol. Excited with picoseconds pulsed 405 nm laser; the decay of emission was monitored at 445 nm. $c = 1.0 \times 10^{-5}$ in MeOH, 20 °C.

lifetime with double exponential decay feature (τ_1 = 0.46 ns, 78%; τ_2 = 4.28 ns, 22%). The lifetime is much shorter than the fluorescence lifetime of perylene (Figure S18, Supporting Information and Table 1). This quenched fluorescence lifetime

Table 1. Photophysical Properties of the Compounds

	λ_{abs} [a]	ε [b]	λ_{em}	Φ_F (%) [c]	τ_F [d] (ns)
Py	406/433	3.11/4.06	437/463	94	4.41/4.72[e]
Py + RSH	406/433	3.11/4.06	436/463	95	4.43/4.71[e]
Py-M	411/438	2.75/3.56	445/471	0.8	3.32[f]/2.82[e]
Py-M + RSH	411/438	2.75/3.56	445/471	97	4.2/4.45[e]

[a]In MeOH ($c = 1.0 \times 10^{-5}$ M). [b]Molar absorption coefficient. ε: 10^4 M^{-1} cm^{-1}. [c]Fluorescence quantum yield in methanol, with perylene as a standard (Φ_F = 94% in *n*-hexane). [d]Fluorescence lifetime in MeOH. [e]In DMSO. [f]Double exponential fitting, with τ_1 = 0.46 ns (relative amplitude: 78%); τ_2 = 4.28 ns (relative amplitude: 22%). This double exponential fitting means the majority of the singlet excited state was quenched by PET.

is assigned due to the PET effect.[39,40] Normally the decay of the fluorescence of a molecule with PET effect shows a short-lived component and a component with longer fluorescence lifetime which is close to the unquenched fluorophore. The charge-transfer quantum yield (Φ_{CT}) was calculated as 89% based on the fluorescence lifetime data (Supporting Information).[39] In the presence of thiols, the fluorescence lifetime was extended to 4.2 ns, which is close to that of perylene. The photophysical parameters of the compounds are summarized in Table 1.

2.3. Redox Properties: Cyclic Voltammogram of the Compounds and the Gibbs Free Energy Changes (ΔG_{CS}°) of the PET process. The electrochemical properties of **Py** and **Py-M** were studied (Figure 4). Perylene shows reversible oxidation wave at +0.58 V. No reduction wave was

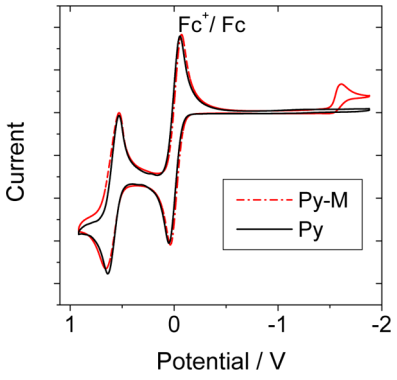

Figure 4. Cyclic voltammogram of the compounds **Py** and **Py-M** (1 mM). Ferrocene (Fc) was used as internal reference. In deaerated CH_2Cl_2 solutions, 0.10 M Bu_4NPF_6 as supporting electrolyte, Ag/$AgNO_3$ reference electrode. Scan rates: 50 mV/s, 20 °C.

observed for perylene up to −1.90 V. For **Py-M**, the oxidation wave is similar (+0.59 V). An irreversible reduction wave was observed at −1.61 V. This reduction wave is attributed to the maleimide moiety, thus it can act as the electron acceptor in the PET process, which is responsible for the quenching of the fluorescence in **Py-M**. We noted the different peak current of the reduction and oxidation peaks of **Py-M**, which may be due to the reversible and the irreversible feature of the two waves. The redox potentials of the compounds were collected in Table 2. We also prepared the thiol adduct of **Py-M**, and the CV curve of the adduct was obtained (Figure S23, Supporting Information). No reduction band was observed for the adduct.

Table 2. Electrochemical Redox Potentials of the Compounds[a]

compound	oxidation (V)	reduction (V)
Py	+0.58	–[b]
Py-M	+0.59	−1.61
Py-M-adduct	+0.38, +0.58	–[b]

[a]Cyclic voltammetry in Ar saturated CH_2Cl_2 containing a 0.10 M Bu_4NPF_6 supporting electrolyte. Counter electrode is Pt electrode, and working electrode is glassy carbon electrode, Ag/$AgNO_3$ couple as the reference electrode. c [Ag^+] = 0.1 M. 0.1 mM compounds in CH_2Cl_2, 25 °C. Ferrocene (Fc) was used as internal reference ($E_{1/2}$ = +0.64 V (Fc^+/Fc) vs standard hydrogen electrode. [b]Not observed.

The Gibbs free energy changes (ΔG_{CS}°) of the intramolecular electron-transfer process of **Py-M** can be calculated with the Weller equation (eqs 1 and 2):

$$\Delta G_{CS}^{\circ} = e[E_{OX} - E_{RED}] - E_{00} + \Delta G_S \quad (1)$$

$$\Delta G_S = -\frac{e^2}{4\pi\varepsilon_S\varepsilon_0 R_{CC}} - \frac{e^2}{8\pi\varepsilon_0}\left(\frac{1}{R_D} + \frac{1}{R_A}\right)\left(\frac{1}{\varepsilon_{REF}} - \frac{1}{\varepsilon_S}\right) \quad (2)$$

where ΔG_S is the static Coulombic energy, which is described by eq 2; e = electronic charge; E_{OX} = half-wave potential for one-electron oxidation of the electron-donor unit, E_{RED} = half-wave potential for one-electron reduction of the electron-acceptor unit; E_{00} = energy level approximated with the fluorescence emission (for the singlet excited state); ε_S = static dielectric constant of the solvent; R_{CC} = center-to-center separation distance between the electron donor and electron acceptor, determined by DFT optimization of the geometry,

DOI: 10.1021/acs.joc.5b02415
J. Org. Chem. 2016, 81, 587−594

R_{CC} (**Py-M**) = 7.10 Å; R_D is the radius of the electron donor; R_A is the radius of the electron acceptor; and ε_{REF} is the static dielectric constant of the solvent used for the electrochemical studies, ε_0 is permittivity of free space. The solvents used in the calculation of free energy of the electron transfer are toluene (ε_S = 2.38), CH_2Cl_2 (ε_S = 8.93), and acetonitrile (ε_S = 37.5).

Energies of the charge-separated states (E_{CS}) and charge recombination energy state (ΔG_{CR}) can be calculated with eqs 3 and 4:

$$E_{CS} = e[E_{OX} - E_{RED}] + \Delta G_S \quad (3)$$

$$\Delta G_{CR} = -(\Delta G_{CS} + E_{00}) \quad (4)$$

We found ΔG_{CS} = −1.05 eV for the PET process in MeOH (Table 3), thus the fluorescence of **Py-M** should be quenched,

Table 3. Driving Forces of Charge Recombination (ΔG_{CR}), Charge Separation (ΔG_{CS}), and Charge Separation Energy States (E_{CS}) of Py-M in Toluene, Dichloromethane, Acetonitrile, and Methanol

	ΔG_{CS} (eV)[a]	ΔG_S[b]	ΔG_{CR}[c]	E_{CTS} (eV)[e]
$PhCH_3$	−0.09	+0.53	−2.72	2.72
CH_2Cl_2	−0.85	−0.23	−1.96	1.96
CH_3CN	−1.06	−0.44	−1.75	1.75
CH_3OH	−1.05	−0.43	−1.76	1.76

[a]Charge separation driving force. [b]Statics Coulombic energy, in eV. [c]Free energy changes of the charge recombination. [d]Energy levels of the charge-transfer state (CTS).

which is in agreement with the experimental results (Figure 2). Thus, the calculation of the Gibbs free energy changes (ΔG_{CS}) supports the PET mechanism for the weak fluorescence of **Py-M**. On the other hand, the energy level of the charge-transfer state (CTS, E_{CTS} = 1.75−2.72 eV, Table 3) of **Py-M** is lower than that of the S_1 state of perylene fluorophore (2.79 eV), indicating that the fluorescence of **Py-M** can be quenched by PET, with maleimide moiety as the electron acceptor. The CV curve of the thiol adduct of **Py-M** (Figure S23, Supporting Information) does not show any reduction peak. This result means the electron acceptor in the adduct vanished, thus the PET was prohibited in the adduct, as a result, the fluorescence recovered.

2.4. Thiol-Activated TTA Upconversion with Py-M as Triplet Acceptor. The thiol-activated TTA upconversion with **Py-M** as the triplet acceptor/emitter was studied with diiodoBodipy as the triplet photosensitizer in deaerated methanol (Figure 5). A 532 nm continuous solid-state laser was used as the light source. For **Py-M** alone, no upconversion was observed (upconversion quantum yield Φ_{UC} = 0%). This result is attributed to the extremely low fluorescence quantum yield of **Py-M** (Φ_F = 0.8%), although the triplet−triplet energy transfer (TTET) may occur (see Intermolecular Triplet−Triplet Energy Transfer (TTET) section). Please note that both efficient TTET and high fluorescence quantum yield of the triplet acceptor are essential for TTA upconversion.[1−4] It should be noted that the emission band at 550 nm is due to the residual fluorescence of the triplet photosensitizer.

In the presence of thiol (2-mercaptoethanol), fluorescence emission bands in the range of 420−525 nm were observed, i.e., the upconverted emission was greatly enhanced (Figure 5a). The upconversion quantum yield (Φ_{UC}) was increased from 0% to 5.9%. This activation effect, or the contrast ratio,[41] is much

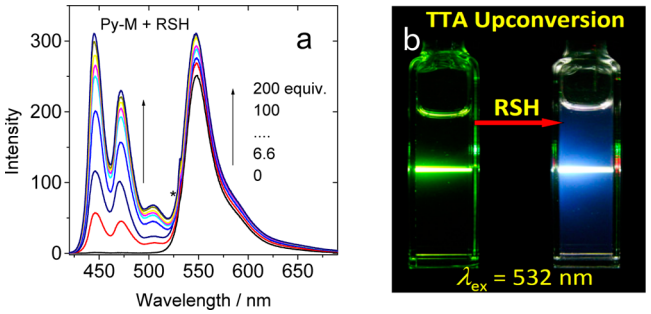

Figure 5. Thiol-activated TTA upconversion with **Py-M** as triplet acceptor/emitter and **B-1** as a photosensitizer. (a) In the presence of 2-mercaptoethanol. (b) Photographs of the thiol-activated upconversion of **Py-M**. Upconversion was performed upon excitation with a 532 nm continuous laser (power density is 24.5 mW cm^{-2}). *c* [**B-1**] = 1.0 × 10^{-5} M, [**Py-M**] = 3.0 × 10^{-5} M ,and [2-mercaptoethanol] = 0.1 M in deaerated methanol, 20 °C.

higher than the previously reported thiol-activatable TTA upconversion,[28] which is based on the DNBS-caged diiodoBodipy triplet photosensitizers. In that system, the cleavage of the DNBS moiety will switch on the upconversion, but the upconversion quantum yield changed only from 0.2% to 0.5%. The reason for the poor switching effect is due to the quenching of the triplet state of the photosensitizer by the side product (electron acceptor) of the cleavage reaction. In the present system (Scheme 2), however, no such "dark" quencher was produced. The activation effect is significant to unaided eyes (Figure 5b). This thiol-activatable TTA upconversion may be useful for in vivo luminescent thiol imaging based on TTA upconversion.[20]

2.5. Intermolecular Triplet−Triplet Energy Transfer (TTET). In order to study the mechanism of the thiol-activated TTA upconversion, the intermolecular TTET between the triplet photosensitizer **B-1** and the triplet acceptor **Py-M** and **Py-M** in the presence of thiol was studied (Figure 6). The aim of this study is to evaluate the difference of the TTET for **Py-M** and **Py-M** + thiol and to investigate the probability of quenching of the triplet state of perylene by PET effect in **Py-M**. The triplet state of perylene, **Py-M** or the **Py-M**/Thiol adduct, was produced by the intermolecular TTET. The perylene derivatives are unable to form a triplet state upon photoexcitation, due to the lack of ISC.

In Figure 6, the decay curves was monitored at two wavelengths, i.e., 520 nm, representing the decay of the triplet state of the triplet donor and 470 nm, representing the production as well as the decay of the triplet state of the energy acceptor. When the mixture of triplet donor (diiodo-Bodipy) and triplet acceptor (**Py**, **Py-M**, or **Py-M** + 2-mercaptoethanol) was excited, the triplet lifetime at 520 nm decreases as compared with that of the triplet energy donor alone (129.3 μs, Figure S22, Supporting Information), indicating the quenching of the triplet state of the photosensitizer. On the other hand, the decay curve at 470 nm indicates the production and then the decay of the triplet state of the energy acceptor. There are two phases for the decay curves monitored at 470 nm: the first rising phase indicates the intermolecular TTET, and the second decreasing phase is the decay of the triplet state.

The results show that the optical density (O.D.) value for the perylene, **Py-M** and **Py-M** + thiol, formed by intermolecular TTET with **B-1** as the triplet energy donor, are same (ΔO.D. =

DOI: 10.1021/acs.joc.5b02415
J. Org. Chem. 2016, 81, 587−594

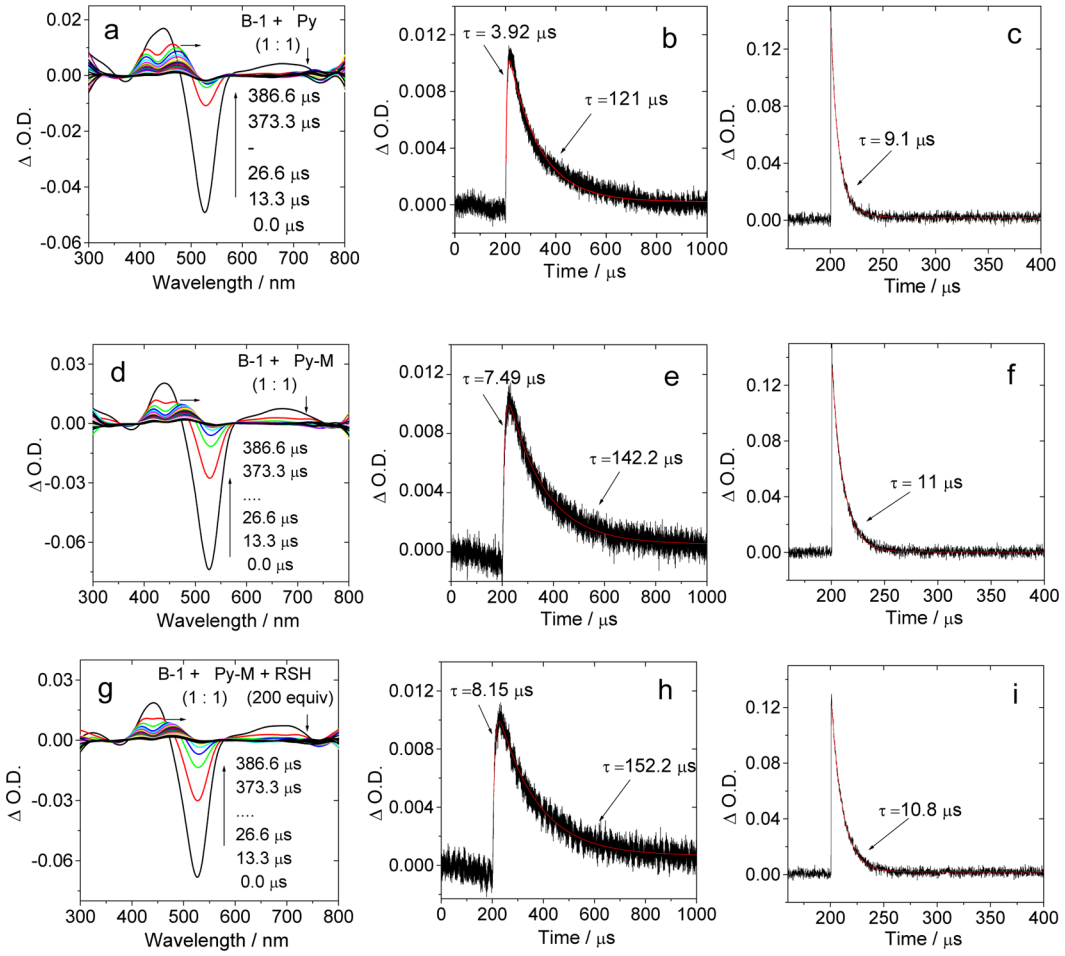

Figure 6. Nanosecond transient absorption spectra of **B-1** in the presence of (a) **Py**, (d) **Py-M**, and (g) **Py-M** with 200 equiv of 2-mercaptoethanol added. (b, e, h) The decay curve of the transient at 470 nm of the mixture of **B-1**/**Py** (1:1), **B-1**/**Py-M** (1:1), and **B-1**/**Py-M** (1:1) with 200 equiv of 2-mercaptoethanol added, respectively. (c, f, i) The decay curve of the transient at 520 nm of the mixture of **B-1**/**Py** (1:1), **B-1**/**Py-M** (1:1), and **B-1**/**Py-M** (1:1) with 200 equiv of 2-mercaptoethanol added, respectively. Excited with 532 nm pulsed laser. Concentration of **B-1**, **Py**, and **Py-M** = 1.0×10^{-5} M, in deaerated MeOH, 20 °C. In order to demonstrate that the triplet state of **B-1** was quenched by **Py** and **Py-M** and the new triplet state formed, the decay traces at 520 and 470 nm were monitored, and the time windows for monitoring of the decay are the same. The ΔO.D. axial in the figures are also the same.

0.01). Thus, we propose the TTET efficiency for perylene, **Py-M** and **Py-M** + thiol are same.

This conclusion is also supported by the quantitative analysis of the quenching, i.e., by studying the Stern−Volmer constant of **Py-M** ($K_{SV} = 1.32 \times 10^6$ M^{-1}) and **Py-M** + thiol ($K_{SV} = 1.31 \times 10^6$ M^{-1}). Moreover, the triplet-state lifetime of **Py**, **Py-M** and **Py-M** + thiol are 121, 144.2, and 152.2 μs, respectively. Thus, we propose that the triplet excited state of the perylene chromophore in **Py-M** was not quenched by any PET, although the fluorescence (S_1 singlet state) of **Py-M** was quenched by PET. Note the energy level of the CTS (E_{CTS} > 1.75 eV, Table 3) is higher than the triplet state of the perylene (1.53 eV). Therefore, the thiol-activated TTA upconversion is due to the thiol-switched fluorescence change of **Py-M**.

The bimolecular quenching constants of the intermolecular TTET processes with different triplet acceptor were calculated (Table 4). In general the k_q values are on the scale of 10^{10} M^{-1} s^{-1}, which are close to the diffusion-controlled bimolecular rate constants in fluid solution at room temperature. This result indicates that the intermolecular TTET is efficient.

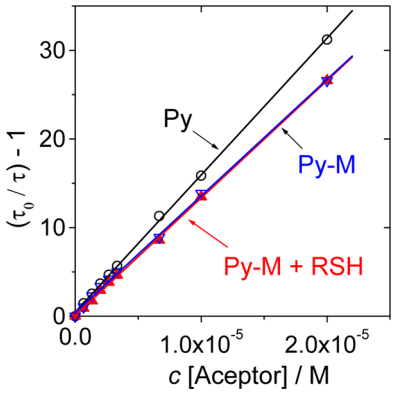

Figure 7. Stern−Volmer plot of quenching of the triplet state of **B-1** with different triplet acceptor. c [triplet photosensitizer] = 1.0×10^{-5} M in deaerated MeOH, 20 °C.

3. CONCLUSION

In summary, thiol-activated TTA upconversion with maleimide-caged perylene fluorophore (**Py-M**) as triplet acceptor/emitter was developed. With diiodoBodipy as the triplet photo-

DOI: 10.1021/acs.joc.5b02415
J. Org. Chem. 2016, 81, 587−594

Table 4. Stern–Volmer Quenching Constant (K_{SV}) and Bimolecular Quenching Constant (k_q) of Compounds Py, Py-M, and Py-M with 200 equiv of 2-Mercaptoethanol[a]

name of compound	K_{SV} 10^6 [M^{-1}]	k_q 10^{10} [M^{-1} s^{-1}]
Py	1.54	1.25
Py-M	1.32	1.03
Py-M + RSH	1.31	1.07

[a]**B-1** was used as photosensitizer. All data were obtained with photosensitizer concentration at 1.0×10^{-5} M in deaerated MeOH solution, 20 °C. Excited with 532 nm laser.

sensitizer, the upconversion can be activated by thiols, and the upconversion quantum yield was increased from 0% to 5.9%, in the presence of thiol such as 2-mercaptoethanol. Our strategy is to cage the fluorescence of perylene with maleimide, by the PET effect, which was confirmed by study of the Gibbs free energy ($\Delta G_{CS}°$) of the PET process. In the presence of thiols, the addition of the thiols to the maleimide moiety at mild condition inhibits the PET, and the adduct shows high fluorescence quantum yield (Φ_F = 97%). Accordingly, the TTA upconversion quantum yield can be switched from 0% to 5.9% in the presence of thiol in deaerated solvent. With E_{CTS} values and nanosecond transient absorption spectroscopy, we found that in stark contrast to the quenching of the singlet excited state, the triplet excited state of the **Py-M** was not quenched by any PET process. This efficient thiol-activatable upconversion and study of the different quenching effect on the singlet and triplet excited state are useful for future development of TTA upconversion and fundamental photochemistry studies of organic chromophores.

4. EXPERIMENTAL SECTION

4.1. Analytical Measurements. All the chemicals used in synthesis are analytical pure and were used as received. Solvents were dried and distilled before used for synthesis. Fluorescence lifetimes were measured on a OB 920 fluorescence/phosphorescence lifetime instrument. Luminescence quantum yields of the compounds were measured in two different solvents with perylene as a standard (Φ_F = 94% in *n*-hexane).

4.2. Synthesis of 3-Formylperylene (1).[42] Perylene (2.52g, 10 mmol) was added to a stirred mixture of anhydrous *o*-dichlorobenzene (5 mL) and anhydrous DMF (4.75 g, 65 mmol), the reaction mixture was heated to 100 °C, $POCl_3$ (3.07 g, 20 mmol) was added dropwise through a dropping funnel over a period of 30 min and then stirred for an additional 4 h at same temperature. The reaction mixture was cooled, put into H_2O (500 mL), and neutralized by dilute aqueous sodium acetate and remained at 0 °C for 3 h. The precipitate was filtered off, washed with H_2O (3 × 30 mL), and purified by column chromatography (silica gel, DCM as eluent). Compound **1** was obtained as orange crystal (1.76 g, 62.8%); mp 233–235 °C; ^{1}H NMR ($CDCl_3$, 400 MHz): δ 10.29 (s, 1H), 9.14 (d, 1H, *J* = 8.0 Hz), 8.28–8.23 (m, 4H), 7.90 (d, 1H, *J* = 8.0 Hz), 7.80 (d, 1H, *J* = 8.0 Hz), 7.73 (d, 1H, *J* = 8.0 Hz), 7.67 (t, 1H, *J* = 8.0 Hz), 7.55–7.50 (m, 2H). TOF HRMS EI$^+$: Calcd ($[C_{21}H_{12}O]^+$), *m*/*z* = 280.0888; found, *m*/*z* = 280.0890.

4.3. Synthesis of 3-Hydroxymethylperylene (2).[42] 1-Formylperylene (400 mg, 1.4 mmol) was dissolved in dry THF:MeOH (50 mL, 2:1, v/v) mixture in flask, and then $NaBH_4$ (162 mg, 4.2 mmol) was added in small portions into the solution. The solution was stirred at RT overnight. The reaction mixture was diluted with CH_2Cl_2 (100 mL), and the solution was washed with brine (100 mL). The organic phase was dried over Na_2SO_4, and solvent was removed under reduced pressure. The residue was purified by column chromatography (silica gel, CH_2Cl_2). Compound **2** was obtained as dark-yellow solid (256 mg, 65%); mp 208–210 °C; ^{1}H NMR ($CDCl_3$, 400 MHz): δ 8.24–8.14 (m, 4H), 7.95 (d, 1H, *J* = 8.0 Hz), 7.69 (d, 2H, *J* = 8.0 Hz), 7.57–7.46 (m, 4H), 5.09 (s, 2H), 1.71 (b, 1H). TOF HRMS EI$^+$: Calcd ($[C_{21}H_{14}O]^+$), *m*/*z* = 282.1045; found, *m*/*z* = 282.1047.

4.4. Synthesis of 3-(Azidomethyl)perylene (3).[43] In a 25 mL flask, hydroxymethylperylene (141 mg, 0.5 mmol) and triphenylphosphine (197 mg, 0.8 mmol) were dissolved in dry DMF (3 mL), and then CBr_4 (249 mg, 0.8 mmol) was added at 0 °C. The solution was stirred for 10 min at 0 °C. Afterward NaN_3 (194 mg, 3 mmol) was added, and slurry was stirred at RT for 24 h. The slurry was diluted with CH_2Cl_2 (100 mL), the solution was washed with water (2 × 80 mL), the organic phase was dried over Na_2SO_4, and solvent was removed under reduced pressure. The crude product was purified by column chromatography (silica gel, hexane/CH_2Cl_2 2:1, v/v). Compound **3** was obtained as a dark green solid (113 mg, 74%); mp 158–160 °C; ^{1}H NMR ($CDCl_3$, 400 MHz): δ 8.26–8.14 (m, 4H), 7.84 (d, 1H, *J* = 8.0 Hz), 7.70 (dd, 2H, *J* = 8.0 Hz), 7.57 (t, 1H, *J* = 8.0 Hz), 7.48 (q, 3H, *J* = 8.0 Hz), 4.71 (s, 2H). TOF HRMS EI$^+$: Calcd ($[C_{21}H_{13}N_3 - N_2]^+$), *m*/*z* = 279.1048; found, *m*/*z* = 279.1052.

4.5. Synthesis of 3-(Aminomethyl)perylene (4). Methanol (120 mL) was purged with argon for 5 min and added to flask containing 3-(azidomethy)perylene (200 mg, 0.65 mmol) and 10% Pd/C (120 mg) under argon atmosphere. The gray yellow mixture was stirred under a hydrogen atmosphere for 16 h. The Pd/C catalyst was filtered through a short silica pad and washed with hot methanol. The filtrate and washing were combined, and methanol was removed under reduced pressure to afford 3-(amiomethyl)perylene in quantitative yield. The crude product was used in next reaction without any purification.

4.6. Synthesis of the Maleimide-Caged Perylene (Py-M). To a stirred solution of maleic anhydride (274 mg, 2.8 mmol) in acetic acid (25 mL) was added 3-(aminomethyl)perylene (200 mg, 0.71 mmol). The reaction mixture was stirred at reflux for 5 h, and then acetic acid was removed under reduced pressure. The residue was dissolved in CH_2Cl_2 (50 mL) and washed with aqueous $NaHCO_3$ (2 × 30 mL). The organic layer was separated and dried (Na_2SO_4), the solvent was removed in vacuum, and the crude product was purified by column chromatography (silica gel, CH_2Cl_2: hexane 1:2). Compound **Py-M** was obtained as dark-orange solid (130 mg, 50% yield) ; mp > 230 °C; ^{1}H NMR ($CDCl_3$, 500 MHz, $CDCl_3$) δ 8.24–8.13 (m, 4H), 8.08 (d, 1H, *J* = 8.0 Hz), 7.68 (d, 2H, *J* = 8.0 Hz), 7.59–7.46 (m, 4H), 6.74 (s, 2H), 5.09 (s, 2H); ^{13}C NMR ($CDCl_3$, 100 MHz, $CDCl_3$) δ 170.6, 134.6, 134.3, 132.4, 131.8, 131.6, 131.1, 130.9, 130.7, 129.0, 128.4, 128.1, 128.0, 127.1, 126.6, 123.1, 120.5, 120.4, 120.3, 119.6, 39.6. TOF HRMS EI$^+$: Calcd ($[C_{25}H_{15}NO_2]^+$), *m*/*z* = 361.1103; found, *m*/*z* = 361.1114.

4.7. Synthesis of the Maleimide-Caged Perylene Adduct. Maleimide-caged perylene **Py-M** (20 mg, 0.05 mmol) was dissolved in mixture of dry DCM:MeOH (30 mL, 1:1, v/v), and then an excessive amount of 2-mercaptoethanol was added into the solution. The solution was stirred at RT for 3 h. The solvent was removed under reduced pressure. The residue was purified by column chromatography (silica gel, CH_2Cl_2: MeOH, 50:1). The adduct was obtained as dark-yellow solid (21 mg, 95%); ^{1}H NMR ($CDCl_3$, 500 MHz): δ 8.24–8.13 (m, 4H), 8.08 (d, 1H, *J* = 10.0 Hz), 7.69 (d, 2H, *J* = 10.0 Hz), 7.58 (d, 2H, *J* = 10.0 Hz), 7.49 (t, 2H, *J* = 10.0 Hz), 5.10 (dd, 2H, *J* = 10.0 Hz), 3.93–3.82 (m, 3H), 3.20 (dd, 1H, *J* = 10.0 Hz), 3.14–3.09 (m, 1H), 2.90–2.84 (m, 2H), 1.85 (b, 1H). TOF HRMS ESI: Calcd ($[C_{27}H_{21}NO_3S - H^+]^-$), *m*/*z* = 438.1168; found, *m*/*z* = 438.1172.

4.8. Nanosecond Time-Resolved Transient Absorption Spectra. The nanosecond time-resolved transient absorption spectra were recorded by Edinburgh LP920 laser flash photolysis spectrometer (Edinburgh Instruments, UK). The signal was digitized on a Tektronix TDS 3012B oscilloscope and analyzed by the LP 900 software. The lifetime values (by monitoring the decay trace of the transients) were obtained with the LP900 software. All the samples in flash photolysis experiments were deaerated with N_2 for ca. 15 min before measurement, and the gas flow is kept during the measurement.

4.9. Cyclic Voltammetry. Cyclic voltammograms were recorded at scan rates of 0.05 V/s. A three-electrodes electrolytic cell was used.

DOI: 10.1021/acs.joc.5b02415
J. Org. Chem. 2016, 81, 587–594

Electrochemical measurements were performed at RT using 0.1 M tetrabutylammonium hexafluorophosphate ($Bu_4N[PF_6]$) as supporting electrolyte, after purging with N_2. The working electrode was a glassy carbon electrode, and the counter electrode was a platinum electrode. A nonaqueous $Ag/AgNO_3$ (0.1 M in acetonitrile) reference electrode was contained in a separate compartment connected to the solution via semipermeable membrane. DCM was used as the solvent. Ferrocene was added as the internal reference.

4.10. TTA Upconversion. A continuous diode pumped solid-state laser (532 nm) was used as the excitation source for the upconversion. The diameter of the laser spot was 3 mm, and power of laser beam was measured with VLP-2000 pyroelectric laser power meter. For the upconversion experiments, the mixed solution of the triplet photosensitizer, triplet acceptor was degassed with N_2 for at least 15 min, and gas flow was kept during the measurement. Then solution was excited with laser, and upconverted fluorescence was recorded with a RF 5301PC spectrofluorometer. In order to repress the laser scattering, a small black box was put behind the fluorescent cuvette to dump the laser.

The upconversion quantum yield (Φ_{UC}) was determined with prompt fluorescence of **B-1** as the standard. The upconversion quantum yield was calculated with following eq 5, where Φ_{UC}, A_{sam}, I_{sam}, and η_{sam} represents the quantum yield, absorbance, integrated photoluminescence intensity, and refractive index of the solvents:

$$\Phi_{UC} = 2\Phi_{Std}\left(\frac{A_{Std}}{A_{unk}}\right)\left(\frac{I_{Std}}{I_{unk}}\right)\left(\frac{\eta_{Std}}{\eta_{unk}}\right) \quad (5)$$

■ ASSOCIATED CONTENT

Supporting Information

The Supporting Information is available free of charge on the ACS Publications website at DOI: 10.1021/acs.joc.5b02415.

General experimental methods, ^1H, ^{13}C NMR data, and HRMS spectra of the compounds and the photophysical data (PDF)

■ AUTHOR INFORMATION

Corresponding Author

*E-mail: zhaojzh@dlut.edu.cn.

Notes

The authors declare no competing financial interest.

■ ACKNOWLEDGMENTS

We thank the NSFC (21273028, 21473020 and 21421005), Program for Changjiang Scholars and Innovative Research Team in University [IRT_13R06] Ministry of Education (SRFDP-20120041130005), the Fundamental Research Funds for the Central Universities (DUT14ZD226), and Dalian University of Technology for financial support (DUT2013TB07).

■ REFERENCES

(1) Singh-Rachford, T. N.; Castellano, F. N. *Coord. Chem. Rev.* **2010**, *254*, 2560−2573.
(2) Zhao, J.; Ji, S.; Guo, H. *RSC Adv.* **2011**, *1*, 937−950.
(3) Ceroni, P. *Chem. - Eur. J.* **2011**, *17*, 9560−9564.
(4) Monguzzi, A.; Tubino, R.; Hoseinkhani, S.; Campione, M.; Meinardi, F. *Phys. Chem. Chem. Phys.* **2012**, *14*, 4322−4332.
(5) Zhou, J.; Liu, Q.; Feng, W.; Sun, Y.; Li, F. *Chem. Rev.* **2015**, *115*, 395−465.
(6) Kang, J.-H.; Reichmanis, E. *Angew. Chem., Int. Ed.* **2012**, *51*, 11841−11844.
(7) To, W.-P.; Chan, K. T.; Tong, G. S. M.; Ma, C.; Kwok, W.-M.; Guan, X.; Low, K.-H.; Che, C.-M. *Angew. Chem., Int. Ed.* **2013**, *52*, 6648−6652.
(8) Peng, J.; Jiang, X.; Guo, X.; Zhao, D.; Ma, Y. *Chem. Commun.* **2014**, *50*, 7828−7830.
(9) Baluschev, S.; Yakutkin, V.; Miteva, T.; Avlasevich, Y.; Chernov, S.; Aleshchenkov, S.; Nelles, G.; Cheprakov, A.; Yasuda, A.; Müllen, K.; Wegner, G. *Angew. Chem., Int. Ed.* **2007**, *46*, 7693−7696.
(10) Duan, P.; Yanai, N.; Kimizuka, N. *Chem. Commun.* **2014**, *50*, 13111−13113.
(11) Askes, S. H. C.; Mora, N. L.; Harkes, R.; Koning, R. I.; Koster, B.; Schmidt, T.; Kros, A.; Bonnet, S. *Chem. Commun.* **2015**, *51*, 9137−9140.
(12) Chen, H.-C.; Hung, C.-Y.; Wang, K.-H.; Chen, H.-L.; Fann, W. S.; Chien, F.-C.; Chen, P.; Chow, T. J.; Hsu, C.-P.; Sun, S.-S. *Chem. Commun.* **2009**, 4064−4066.
(13) Turshatov, A.; Busko, D.; Avlasevich, Y.; Miteva, T.; Landfester, K.; Baluschev, S. *ChemPhysChem* **2012**, *13*, 3112−3115.
(14) Cui, X.; Charaf-Eddin, A.; Wang, J.; Le Guennic, B.; Zhao, J.; Jacquemin, D. *J. Org. Chem.* **2014**, *79*, 2038−2048.
(15) McCusker, C. E.; Castellano, F. N. *Chem. Commun.* **2013**, *49*, 3537−3539.
(16) Deng, F.; Blumhoff, J.; Castellano, F. N. *J. Phys. Chem. A* **2013**, *117*, 4412−4419.
(17) Cheng, Y. Y.; Khoury, T.; Clady, R. G. C. R.; Tayebjee, M. J. Y.; Ekins-Daukes, N. J.; Crossley, M. J.; Schmidt, T. W. *Phys. Chem. Chem. Phys.* **2010**, *12*, 66−71.
(18) Murakami, Y.; Kikuchi, H.; Kawai, A. *J. Phys. Chem. B* **2013**, *117*, 2487−2494.
(19) Jankus, V.; Snedden, E. W.; Bright, D. W.; Whittle, V. L.; Williams, J. A. G.; Monkman, A. *Adv. Funct. Mater.* **2013**, *23*, 384−393.
(20) Liu, Q.; Yang, T.; Feng, W.; Li, F. *J. Am. Chem. Soc.* **2012**, *134*, 5390−5397.
(21) Monguzzi, A.; Braga, D.; Gandini, M.; Holmberg, V. C.; Kim, D. K.; Sahu, A.; Norris, D. J.; Meinardi, F. *Nano Lett.* **2014**, *14*, 6644−6650.
(22) Lissau, J. S.; Gardner, J. M.; Morandeira, A. *J. Phys. Chem. C* **2011**, *115*, 23226−23232.
(23) Khnayzer, R. S.; Blumhoff, J.; Harrington, J. A.; Haefele, A.; Deng, F.; Castellano, F. N. *Chem. Commun.* **2012**, *48*, 209−211.
(24) Askes, S. H. C.; Bahreman, A.; Bonnet, S. *Angew. Chem., Int. Ed.* **2014**, *53*, 1029−1033.
(25) Cui, X.; Zhao, J.; Zhou, Y.; Ma, J.; Zhao, Y. *J. Am. Chem. Soc.* **2014**, *136*, 9256−9259.
(26) Xu, K.; Zhao, J.; Cui, X.; Ma, J. *Chem. Commun.* **2015**, *51*, 1803−1806.
(27) Ma, J.; Cui, X.; Wang, F.; Wu, X.; Zhao, J.; Li, X. *J. Org. Chem.* **2014**, *79*, 10855−10866.
(28) Zhang, C.; Zhao, J.; Cui, X.; Wu, X. *J. Org. Chem.* **2015**, *80*, 5674−5686.
(29) Tao, R.; Zhao, J.; Zhong, F.; Zhang, C.; Yang, W.; Xu, K. *Chem. Commun.* **2015**, *51*, 12403−12406.
(30) Chen, X.; Zhou, Y.; Peng, X.; Yoon, J. *Chem. Soc. Rev.* **2010**, *39*, 2120−2135.
(31) Wang, F.; Zhou, L.; Zhao, C.; Wang, R.; Fei, Q.; Luo, S.; Guo, Z.; Tian, H.; Zhu, W.-H. *Chem. Sci.* **2015**, *6*, 2584−2589.
(32) Lee, H. Y.; Choi, Y. P.; Kim, S.; Yoon, T.; Guo, Z.; Lee, S.; Swamy, K. M. K.; Kim, G.; Lee, J. Y.; Shin, I.; Yoon, J. *Chem. Commun.* **2014**, *50*, 6967−6969.
(33) Guo, Z.; Nam, S.; Park, S.; Yoon, J. *Chem. Sci.* **2012**, *3*, 2760−2765.
(34) Zhang, H.; Zhang, C.; Liu, R.; Yi, L.; Sun, H. *Chem. Commun.* **2015**, *51*, 2029−2032.
(35) Kand, D.; Mandal, P. S.; Saha, T.; Talukdar, P. *RSC Adv.* **2014**, *4*, 59579−59586.
(36) Matsumoto, T.; Urano, Y.; Shoda, T.; Kojima, H.; Nagano, T. *Org. Lett.* **2007**, *9*, 3375−3377.
(37) Maeda, H.; Maeda, T.; Mizuno, K.; Fujimoto, K.; Shimizu, H.; Inouye, M. *Chem. - Eur. J.* **2006**, *12*, 824−831.
(38) de Silva, A. P.; Gunaratne, H. Q. N.; Gunnlaugsson, T.; Huxley, A. J. M.; McCoy, C. P.; Rademacher, J. T.; Rice, T. E. *Chem. Rev.* **1997**, *97*, 1515−1566.

DOI: 10.1021/acs.joc.5b02415
J. Org. Chem. 2016, 81, 587−594

(39) D'Souza, F.; Chitta, R.; Ohkubo, K.; Tasior, M.; Subbaiyan, N. K.; Zandler, M. E.; Rogacki, M. K.; Gryko, D. T.; Fukuzumi, S. *J. Am. Chem. Soc.* **2008**, *130*, 14263−14272.
(40) Zhang, X.-F.; Wang, J. *J. Phys. Chem. A* **2011**, *115*, 8597−8603.
(41) Cody, J.; Mandal, S.; Yang, L.; Fahrni, C. J. *J. Am. Chem. Soc.* **2008**, *130*, 13023−13032.
(42) Garg, K.; Majumder, C.; Nayak, S. K.; Aswal, D. K.; Gupta, S. K.; Chattopadhyay, S. *Phys. Chem. Chem. Phys.* **2015**, *17*, 1891−1899.
(43) Printz, M.; Richert, C. *Chem. - Eur. J.* **2009**, *15*, 3390−3402.

DOI: 10.1021/acs.joc.5b02415
J. Org. Chem. 2016, 81, 587−594